

# Morphological and optical characterization of GaN prepared by pulsed laser deposition

C. Vinegoni <sup>a,\*</sup>, M. Cazzanelli <sup>b</sup>, A. Trivelli <sup>a</sup>, G. Mariotto <sup>c</sup>, J. Castro <sup>d</sup>, J.G. Lunney <sup>d</sup>, J. Levy <sup>a</sup>

<sup>a</sup> Department of Physics and Astronomy, University of Pittsburgh, Pittsburgh, PA, USA

<sup>b</sup> Group of Applied Physics, University of Geneva, Geneva, Switzerland

<sup>c</sup> INFN and Dipartimento di Fisica, Università di Trento, Trento, Italy

<sup>d</sup> Department of Physics, Trinity College, Dublin 2, Ireland

Received 1 September 1999; accepted 29 November 1999

## Abstract

GaN films were grown by pulsed laser deposition (PLD) on different crystalline substrates using a KrF excimer laser to ablate a hexagonal phase GaN target in a reactive atmosphere of ammonia. Films with small homogeneously distributed granular structures over the entire sample surface were obtained. The microstructure and surface morphology of the deposited layers were characterized by X-ray diffraction (XRD), atomic force microscopy (AFM) and Raman spectroscopy (RS). XRD reveals that the structure of the GaN layer is predominantly wurtzite. AFM images reveal that all the deposited layers have a relatively smooth surface, while RS confirmed the predominant presence of hexagonal GaN with a high polycrystalline character. Analysis of the results obtained for samples grown under different conditions, such as the substrate temperatures in the growth chamber as well as different substrates used, helps to define better the experimental conditions of the growth process of PLD-GaN films. © 2000 Elsevier Science S.A. All rights reserved.

**Keywords:** GaN; Optical properties; Pulsed laser deposition

## 1. Introduction

Gallium nitride (GaN) is one of the most promising semiconductor materials for optoelectronic applications such as light emitting diodes (LEDs) [1–4] and laser systems emitting from blue to ultraviolet [5,6]. After the recent achievement of laser emission at room temperature from GaN [2], a strong research effort has been devoted to understand better the basic properties of this material as well as to improve the growth of thin films. At present, the most widely used growth methods for GaN are metal–organic chemical vapor deposition [6] (MOCVD) and molecular beam epitaxy [7–9] (MBE). Compared with other III–V semiconductors, such as GaAs, films of GaN grown by MOCVD and MBE have a relatively high defect concentration. Recently, pulsed

laser deposition (PLD) has been used to grow GaN films with good crystalline quality and superior optical properties [10–14]. Previously [15,16] we have reported studies on the origin of the recombination processes in GaN films prepared by pulsed laser deposition (PLD-GaN); there we attributed the typical luminescence of PLD-GaN to excitons localized at extended defects. In this paper, we report on the results of comparative investigations of the microstructure and of surface morphology of PLD-GaN films grown on different substrates and with different growth conditions.

## 2. Sample and experimental details

The samples were grown under different conditions (see Table 1); all of them were obtained from GaN powder (nominally 99.99% pure) pressed at room temperature and  $7 \times 10^4 \text{ N cm}^{-2}$ . The target pellet was then sintered for 12 h at 620°C in an N<sub>2</sub> atmosphere (1270 mbar at regime temperature) in order to improve

\* Corresponding author. Tel.: +41-22-726882; fax: +41-22-726882. On leave to: University of Geneva, Group of Applied Physics, 20, Rue de L'Ecole de Medicine, Geneva, Switzerland.

E-mail addresses: claudio.vinegoni@physics.unige.ch (C. Vinegoni), massimo.cazzanelli@unige.ch (M. Cazzanelli)

Table 1

List of the samples prepared and studied. All the films were deposited with the 248 nm wavelength of an KrF excimer laser, operated at 10 Hz and focused with different values of fluence. For all the samples the distance between the sample and the target was 3.5 cm. In the table are reported the varying parameters used in the PLD chamber in order to deposit the films (substrate on which the films were deposited, temperature of the substrate, gas pressure inside the chamber and fluence, respectively)

Sample name	Substrate	Temperature (K)	Pressure (mbar)	Fluence ( $\text{J cm}^{-2}$ )
VIS7	Si(100)	700	0.1	6.0
VIS8	Si(100)	730	0.15	6.0
VIS10	Si(111)	800	0.1	5.4
VIS11	$\text{Al}_2\text{O}_3$	800	$6 \times 10^{-3}$	6.0
VIS12	$\text{Al}_2\text{O}_3$	800	$2 \times 10^{-3}$	4.0
NH3	$\text{Al}_2\text{O}_3$	800	$2 \times 10^{-3}$	6.0

its mechanical strength. The laser ablation was done with the 248 nm wavelength of a KrF excimer laser, operated at 10 Hz and focused to give a fluence on the target variable from 4.0 to 6.0  $\text{J cm}^{-2}$ . The substrates (Si(100), Si(111),  $\text{Al}_2\text{O}_3$  (11 $\bar{2}$ 0)) were placed in turn at about 3.5 cm from the target and maintained at a constant temperature during the growth process. The substrate temperature was varied depending on the sample ranging from 700°C for Si to 800°C for  $\text{Al}_2\text{O}_3$ . The chamber was filled with ammonia in order to support stoichiometric growth. All the growth parameters are reported in Table 1. For the films grown on sapphire, the ammonia pressure was lower than that used in an earlier study [15,16]. X-ray diffraction patterns of the films were recorded using a commercial diffractometer operated in the  $\theta/2\theta$  mode. A conventional tube with copper anode (Cu  $\text{K}\alpha$  radiation) was used as the X-ray source. The measurements were performed at room temperature (RT) in the angle range  $2\theta=(10\text{--}100)^\circ$  and a maximum resolution of about  $10''$ .

The surface morphology of PLD-GaN films was investigated with a home-built atomic force microscope, operated in air at room temperature. Images were acquired using tapping mode with a vertical resolution better than 1 nm. A silicon cantilever with a resonant frequency of  $\sim 275$  kHz and a spring constant of  $42 \text{ N m}^{-1}$  was used. The average surface roughness for each sample was defined as the root mean square (rms) of the deviation from the mean height in the scanned area. For each sample we collected at least five scans on different randomly selected areas and no significant topographic difference was observed among the various scans. Before taking the atomic force microscopy (AFM) measurements, all samples were cleaned with acetone and some droplets of  $\text{H}_2\text{O}$  put on their surface in order to prevent sedimentation during the evaporation of the acetone. The water was evaporated under a flux of nitrogen. The AFM images hereafter presented, were taken from regions with areas equal to 3.24 and  $0.64 \mu\text{m}^2$ , respectively.

The Raman measurements were performed in back-scattering geometry using a micro-probe set-up [17]

consisting of an Olympus microscope (model BHSM-L-2), with a  $100\times$  objective with a numerical aperture  $\text{NA}=0.95$ . This objective allowed us simultaneously to focus the incident radiation on an area of approximately  $1 \mu\text{m}^2$  and to collect the scattered light to be sent to the monochromator. To identify the Raman nature of the spectral features, the laser lines of an  $\text{Ar}^+$  laser (488.0 and 514.5 nm) were used for excitation. All the measurements were performed at room temperature. In order to avoid the heating of the samples the laser power was kept below 80 mW. The microprobe set-up was coupled to a 1 m focal length Jobin-Yvon double monochromator (Ramanor, model HG2-S) equipped with holographic gratings (2000 grooves  $\text{mm}^{-1}$ ). The spectral resolution was approximately  $3 \text{ cm}^{-1}$ . The scattered radiation was detected by a cooled ( $-35^\circ\text{C}$ ) photomultiplier tube (RCA, model C31034A-02) operated in photon counting mode. The signal was stored into a multichannel analyzer and then sent to a computer for analysis.

### 3. Experimental results

#### 3.1. XRD and AFM

The films have a thickness which we estimate to be between 150 nm for the samples grown on sapphire, and 300 nm for the sample grown on silicon. The XRD patterns obtained from the different PLD-GaN samples indicate that the structure of the films consists of a single phase characterized by a strong peak at  $2\theta=34.4^\circ$  associated with the reflection from (0002) planes of hexagonal GaN, even for the films grown on Si. A typical XRD spectrum of a film deposited on  $\text{Al}_2\text{O}_3$  (sample VIS11) in the  $\theta/2\theta$  configuration is shown in Fig. 1(a). The peaks at  $2\theta=34.4^\circ$  and at  $2\theta=72.9^\circ$  are respectively ascribed to the (0002) and (0004) planes of wurtzitic GaN [18–21]. This shows that these films are strongly textured with the  $c$ -axis normal to the film plane. The two most intense diffraction peaks are the reflections from the (11 $\bar{2}$ 0)  $\text{Al}_2\text{O}_3$  substrate, while the

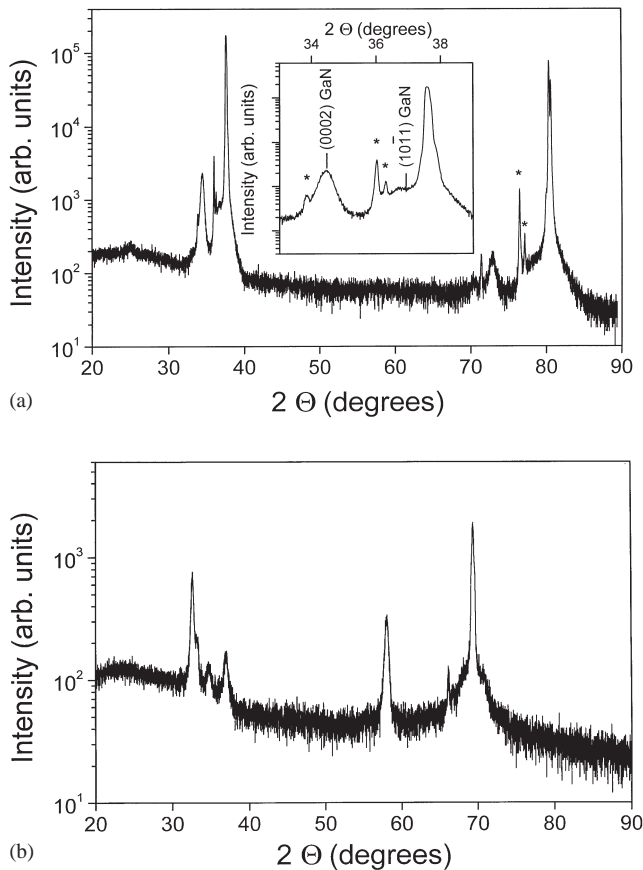


Fig. 1. (a) XRD spectrum for a typical GaN sample grown on  $\text{Al}_2\text{O}_3$  (VIS11). The XRD features marked with an asterisk are due to anode contamination of the tungsten cathode. In the inset is shown the part of the XRD pattern on an expanded scale. (b) XRD spectrum for a Si-grown sample (VIS7).

narrow peaks marked with an asterisk are ascribed to tungsten contamination at the copper anode. All the peaks found and their attribution are given in Table 2. In Fig. 1(b) is shown a representative XRD spectra

Table 2

In the table are reported the position of the peaks for the XRD spectra taken on sample VIS11. The theoretical values are taken from JCPDS-ICDD; #42-1468 for  $\text{Al}_2\text{O}_3$  and #6-503 for a-GaN. The attributions are made in accordance with them

VIS11	Attributed			
	$2\theta$ (Exp.)	$2\theta$ (Theor.)	(hkl)	Phase
	33.8	33.8	0002	GaN <sup>a</sup>
	34.4	34.6	0002	GaN
	36.0/36.3	36.2/36.4	$11\bar{2}0$	$[\text{Al}_2\text{O}_3]^a$
	36.7	37.0	$10\bar{1}1$	GaN
	37.6	37.8	$11\bar{2}0$	$\text{Al}_2\text{O}_3$
	72.9	73.0	0004	GaN
	76.5	76.4	$22\bar{4}0$	$[\text{Al}_2\text{O}_3]^a$
	77.2/77.8	77.2	$22\bar{4}0$	$[\text{Al}_2\text{O}_3]^a$
	80.0/80.7	80.6	$22\bar{4}0$	$\text{Al}_2\text{O}_3$

<sup>a</sup> Peaks due to tungsten contamination at the copper anode.

taken on one of the three films grown on silicon (sample VIS7). The main peaks (in order of decreasing intensity) are ascribed to the  $(11\bar{2}2)$ ,  $(10\bar{1}0)$ ,  $(11\bar{2}0)$ ,  $(10\bar{1}1)$  and  $(0002)$  planes of wurtzitic GaN. The peak positions and attributions are summarized in Table 3.

Fig. 2(a) and (b) shows the AFM scan images observed from samples VIS7 and VIS11, respectively. The images show the height profile at half vertical axis, along the horizontal axis. The RMS surface roughness (30 and 45 nm for sample VIS7 and VIS11, respectively) indicates a relatively smooth surface for all the deposited films. All the samples show a granular surface with features of about 100 nm. The AFM images of the films deposited under different conditions are quite similar. The surface of all the samples is featureless with small granular structures that have a mean size of roughly 100 nm. In some cases we observed some circular structures with a diameter of  $\sim 2\ \mu\text{m}$  superimposed on a uniform background of smaller crystallites; these structures are probably due to the deposition of GaN particulates, which often arises in PLD [22].

### 3.2. Raman spectroscopy

The XRD spectra show that our GaN films have the hexagonal wurtzite structure. Hexagonal GaN belongs to the space group  $C_{6v}^4$  with two formula units per unit cell [23]. In accordance with the factor group analysis the optical phonons of hexagonal GaN at the G point of the first Brillouin zone belong to the following irreducible representations [24]:

$$\Gamma_{\text{opt}} = A_1(Z) + 2B + E_1(X, Y) + 2E_2, \quad (1)$$

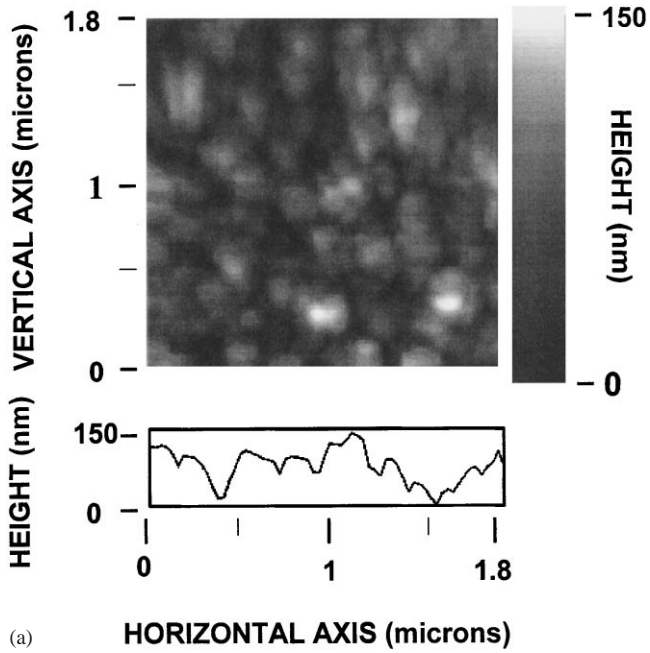
where the  $X$ ,  $Y$  and  $Z$  inside the parentheses represents the polarization directions. The Raman active modes belong to the  $A_1$ ,  $E_1$  and  $E_2$  representations. A detailed polarization analysis of Raman scattering from wurtzitic GaN has been reported by Tabata et al. [23] and Azuhata et al. [24]. The phonon frequencies of wurtzitic

Table 3

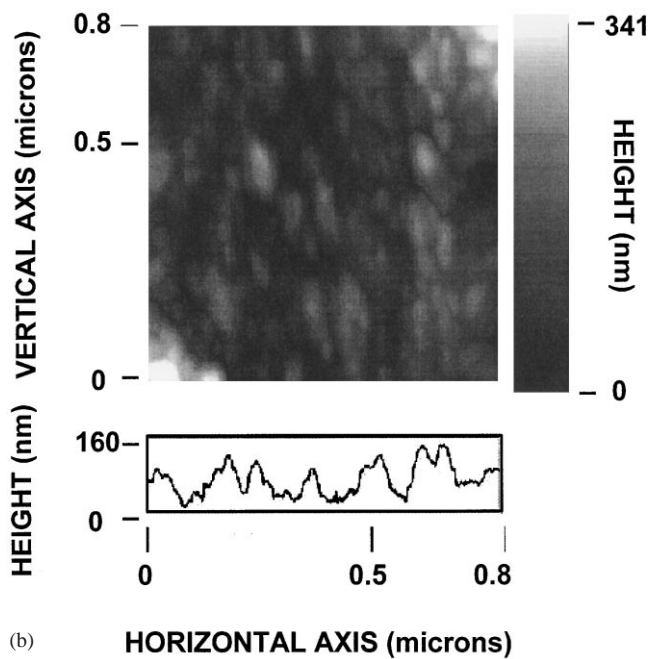
In the table are reported the position of the peaks for the XRD spectra taken on sample VIS7. The theoretical values are taken from JCPDS-ICDD #6-503 for a-GaN. The attributions are made in accordance with them

VIS7	Attributed			
	$2\theta$ (Exp.)	$2\theta$ (Theor.)	(hkl)	Phase
	32.5	32.4	$10\bar{1}0$	GaN
	33.2	33.3/33.8	–	Si <sup>a</sup>
	34.7	34.6	0002	GaN
	36.9	37.0	$10\bar{1}1$	GaN
	58.0	57.9	$11\bar{2}0$	GaN
	69.3	69.2	$11\bar{2}2$	GaN

<sup>a</sup> A peak that may be due to tungsten contamination at the copper anode.



(a)



(b)

Fig. 2. AFM scan images for sample VIS7 (a) and sample VIS11 (b). On the bottom of the figure is reported the height profile taken at half vertical scan along the horizontal axis.

GaN are observed to depend slightly on the growth procedures followed to deposit the films [23–26].

The Raman spectra recorded from the different PLD-GaN films consist of peaks characteristic of the wurtzite phase. Fig. 3 shows the experimental Raman spectra recorded from two films grown on  $\text{Al}_2\text{O}_3(11\bar{2}0)$  (VIS11) (spectrum b) and Si (100) (VIS7) (spectrum c) sub-

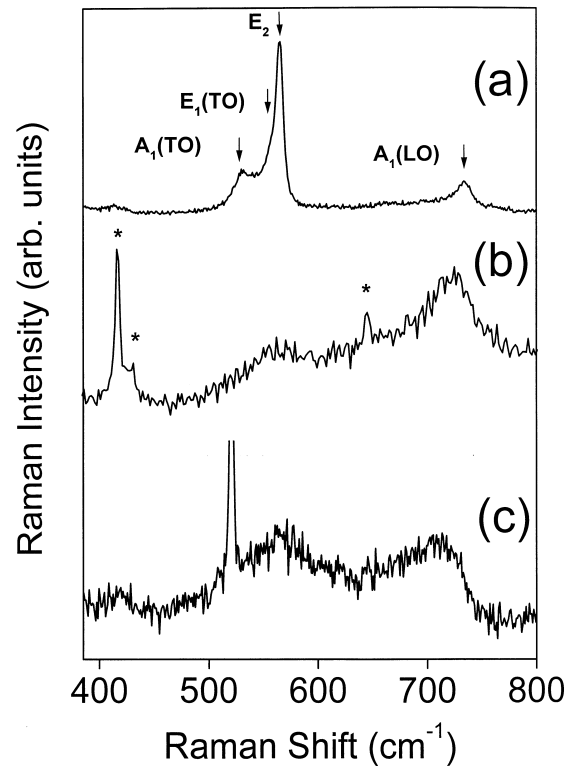


Fig. 3. Micro-Raman spectra of GaN samples carried out at room temperature under excitation of the 488.0 nm  $\text{Ar}^+$  laser line, from: (a) sintered powder used as target to grow PLD-GaN films; (b) sample VIS11 grown on  $\text{Al}_2\text{O}_3(11\bar{2}0)$  substrate; (c) sample VIS7 deposited on crystalline Si(100). The luminescence background was subtracted in all the spectra. The sharp peaks at 418, 432 and 645  $\text{cm}^{-1}$  (marked with an asterisk) of spectrum (b) are due to the sapphire substrate ( $A_{1g}$ ,  $E_g$  and  $A_{1g}$  symmetry), while the strong peak at 520  $\text{cm}^{-1}$  in spectrum (c) is due to c-Si. All the spectra shown were taken on the homogeneous area of the films and not on the particulates.

strates, respectively, and the reference spectrum (spectrum a) obtained from the GaN target made by pressing and sintering the GaN powder.

From the spectrum of Fig. 3(a) that refers to the target material we can easily identify the vibrational modes corresponding to the wurtzitic GaN [26]. The only mode that cannot be resolved is that corresponding to the  $E_1$  (LO) phonon, probably because of its weak intensity. The phonon frequencies of transverse optic (TO)  $A_1$  and  $E_1$  modes and of  $E_2$  mode occur at 530, 557 and 565  $\text{cm}^{-1}$ , respectively, while the longitudinal optic (LO)  $A_1$  is peaked at 734  $\text{cm}^{-1}$ . No symmetry study of Raman scattering from this reference sample was possible since the target pellet consisted of randomly oriented crystalline grains.

Raman spectra recorded from the samples VIS11 (spectrum b) and VIS7 (spectrum c) show two broad bands peaked at 563 and 726  $\text{cm}^{-1}$ . The asymmetry and the small red shift in their positions (compared with the peaks in Fig. 3(a)), suggests that the films have the wurtzite structure, as confirmed from the XRD spectra,

but on a low order phase with an increasing distance in the atomic bonds. Stress effects due to lattice mismatch can be excluded because the peaks positions are the same for every substrate used. Besides these peaks, an additional band centered at about  $420\text{ cm}^{-1}$ , has been observed in all the spectra recorded from PLD samples. This band, not present either in the GaN hexagonal phase or in its cubic phase, has recently been reported for ion-implanted GaN [27] and attributed to vibrational modes of vacancy-related defects. Both the spectra provide evidence that the GaN phase is highly disordered with a small crystallite size suggesting the polycrystalline character of our films. This is confirmed by the appearance of the new band at  $420\text{ cm}^{-1}$  (see Limmer et al. [27]). Moreover a comparison between the spectra of Fig. 3(b) and (c) shows that the films grown on silicon present a higher crystalline quality in accordance with XRD spectra. This is indicated by a decrease in the intensity ratio between the  $726$  and  $563\text{ cm}^{-1}$  band.

#### 4. Summary and conclusion

A spectroscopic characterization of PLD-GaN films grown on different crystalline substrates under a low-pressure ammonia atmosphere [28] has been achieved by adopting a multi-technique approach. XRD patterns show that all our PLD-GaN samples have a predominantly hexagonal phase, suggesting that PLD is a technique which yields preferentially the most stable polytype of the material. The films grown on  $\text{Al}_2\text{O}_3$  present a higher degree of polycrystallinity evidenced by the large width of the attributed GaN planes reflections. The film grown on silicon presents instead a better crystallinity, judging by the appearance of more plane reflections and by the narrowing of the XRD peaks. Moreover the films grown on sapphire are strongly textured with the  $c$ -axis normal to the film plane, while the films on silicon do not show this texturing. AFM scans showed that the surface morphology was very similar for all of the different deposited films. The RMS roughness was about between 30 and 50 nm, suggesting that further work is necessary to improve the surface quality of PLD-GaN films for device applications. Like XRD, Raman spectroscopy also shows that the films are wurtzitic and indicates their low degree of crystallinity. The appearance of a new broad peak at  $420\text{ cm}^{-1}$  is attributed to the presence of vacancy-related defects. The reason for the presence of such a polycrystalline character in our films has to be ascribed to the uncontrolled incorporation of impurities during the growing process and this is in agreement with previous electrical measurements [29]. We do not exclude the presence of some  $\text{Ga}_2\text{O}_3$  in the  $\alpha$  phase. The very similar XRD patterns for  $\text{Ga}_2\text{O}_3$  (JCPDF-ICDD 6-503) and GaN (JCPDF-ICDD 2-1078), where the XRD peaks

of  $\text{Ga}_2\text{O}_3$  have the highest intensity, have not allowed us to resolve the XRD peaks for the different phases. Further investigations concerning this feature are needed, and a photoluminescence study of the set of sample is planned for the near future.

#### Acknowledgements

The authors wish to acknowledge that the software for Raman data acquisition was developed by Dr. E. Zanghellini. M.C. gratefully acknowledges a private communication from R.D. Vispute. Special thanks are due to Ms. C. Armellini, and R.P. Borges.

#### References

- [1] S. Nakamura, M. Senoh, N. Iwasa, S. Nagahama, *Appl. Phys. Lett.* 67 (1995) 1868.
- [2] S. Nakamura, T. Mukai, M. Senoh, *Appl. Phys. Lett.* 64 (1994) 1687.
- [3] D.B. Eason, Z. Yu, W.C. Hughes, C. Boney, J.W. Cook Jr., J.F. Schetzina, D.R. Black, G. Catwell, W.C. Harsh, *J. Vac. Sci. Technol. B* 13 (1995) 4.
- [4] J.W. Yang, Q. Chen, C.J. Sun, B. Lim, M.Z. Anwar, M. Asif Khan, H. Temkin, *Appl. Phys. Lett.* 69 (1996) 369.
- [5] S. Nakamura, M. Senoh, N. Iwasa, S. Nagahama, *Jpn. J. Appl. Phys.* 34 (1995) L979.
- [6] S. Nakamura, M. Senoh, S. Nagahama, N. Iwasa, T. Yamada, T. Matsushita, H. Kiyoku, Y. Sugimoto, *Jpn. J. Appl. Phys.* 35 (1996) L74.
- [7] T. Lei, M. Fanciulli, R.J. Molnar, T.D. Moustakas, R.J. Granham, J. Scanlon, *Appl. Phys. Lett.* 59 (1991) 944.
- [8] C.G. Van de Walle, *Wide-band-gap Semiconductors*, North-Holland, Amsterdam, 1992.
- [9] R. Dwilinski, R. Doradzinski, J. Garczynski, L. Sierzputowski, J.M. Baranowski, M. Kaminska, *Mater. Sci. Eng. B* 50 (1997) 46.
- [10] P. Verardi, M. Dinescu, C. Gerardi, L. Mirengi, V. Sandu, *Appl. Surf. Sci.* 109–110 (1997) 371.
- [11] A.G. Guidoni, A. Mele, R. Teghi, V. Marotta, S. Orlando, A. Santagata, *Appl. Surf. Sci.* 109–110 (1997) 533.
- [12] M.G. Norton, P.G. Kotula, C.B. Carter, *J. Appl. Phys.* 70 (1991) 2871.
- [13] R.F. Xiao, H.B. Liao, N. Cue, X.W. Sun, H.S. Kwok, *J. Appl. Phys.* 80 (1996) 4226.
- [14] D. Cole, J.G. Lunney, F.P. Logue, J.F. Donegan, J.M.D. Coey, *Mater. Sci. Eng. B* 48 (1997) 239.
- [15] M. Cazzanelli, C. Vinegoni, J.G. Lunney, K.P. O'Donnell, P.G. Middleton, C. Trager-Cowan, L. Pavesi, *Mater. Sci. Eng. B* 59 (1999) 137.
- [16] M. Cazzanelli, D. Cole, J.F. Donegan, J.G. Lunney, P.G. Middleton, K.P. O'Donnell, C. Vinegoni, L. Pavesi, *Appl. Phys. Lett.* 73 (1998) 3390.
- [17] A. Kuzmin, J. Purans, E. Cazzanelli, C. Vinegoni, G. Mariotto, *J. Appl. Phys.* 84 (1998) 5515.
- [18] T.S. Cheng, L.C. Jenkins, S.E. Hooper, C.T. Foxon, J.W. Orton, D.E. Lacklison, *Appl. Phys. Lett.* 66 (1995) 1509.
- [19] H. Okumura, S. Misawa, S. Yoshida, *Appl. Phys. Lett.* 59 (1991) 1058.
- [20] S. Fujieda, Y. Matsumoto, *Jpn. J. Appl. Phys.* 30 (1991) L1665.
- [21] D.E. Lacklison, J.W. Orton, I. Harrison, T.S. Cheng, L.C. Jenkins, C.T. Foxon, S.E. Hooper, *J. Appl. Phys.* 78 (1995) 1838.

- [22] D. Cole, J.G. Lumme, J.M.D. Coey, *J. Magn. Magn. Mater.* 165 (1997) 246.
- [23] A. Tabata, R. Enderlin, J.R. Leite, S.W. da Silva, J.C. Galzerani, D. Shikora, M. Kloidt, K. Lischka, *J. Appl. Phys.* 79 (1996) 4137.
- [24] T. Azuhata, T. Sota, K. Suzuki, S. Nakamura, *J. Phys. C* 7 (1995) L129.
- [25] A. Cingolani, M. Ferrara, M. Lugara, G. Scamarcio, *Solid State Commun.* 58 (1986) 823.
- [26] H. Siegle, L. Eckey, A. Hoffmann, C. Thomsen, B.K. Meyer, D. Schikora, M. Hankeln, K. Lischka, *Solid State Commun.* 96 (1995) 943.
- [27] W. Limmer, W. Ritter, R. Sauer, B. Menshing, C. Liu, B. Rauschenbach, *Appl. Phys. Lett.* 72 (1998) 2589.
- [28] R.D. Vispute, personal communication
- [29] M. Cazzanelli, D. Cole, J. Versluijs, J. Donegan, J.G. Lunney, *Mater. Sci. Eng. B* 59 (1999) 162.